

Enhancement of the laser-induced excitation probability of the hyperfine ground state of muonic hydrogen by a multipass cavity setup

Rakesh Mohan Das^{1,2*} and Masahiko Iwasaki³

¹*School of Applied Sciences, KIIT University, Patia,
Bhubaneswar, 751024, Odisha, India.

²Center of Excellence in High Energy and Condensed Matter Physics, Department of Physics, Utkal University, Vani Vihar, Bhubaneswar, 751004, Odisha, India.

³The Institute of Physical and Chemical Research, RIKEN, 2-1
Hirosawa, Wako, Saitama, 351-0198, , Japan.

*Corresponding author(s). E-mail(s): rakesh.dasfpy@kiit.ac.in;

Abstract

We study the enhancement of the magnetic dipole induced excitation probability of the hyperfine ground state of Doppler-broadened muonic hydrogen ($p\mu^-$) by a nanosecond laser pulse in the mid-infrared range with Gaussian temporal shape such that the pulse bandwidth is broader than the Doppler width at 10 K. The enhancement is achieved by shrinking the cross-section of the laser pulse and placing the muonic hydrogen medium in a multipass cavity, while preserving the total irradiated target volume. We numerically solve a set of Maxwell-Schrödinger equations to obtain the excitation probability and the total efficiency for various densities of the muonic hydrogen atomic medium and at various positions in the multipass cavity. For the typical range of densities of muonic hydrogen atoms at major proton accelerator facilities such as the J-PARC (density $\sim 10^5 \text{ cm}^{-3}$), the laser propagation effect is insignificant. For such cases, the total efficiency increases by an order of two for 100 reflections with a uniform polarization. If the density exceeds the value of 10^{17} cm^{-3} as might be in the future advances, the laser propagation effect has to be taken into account, and the total efficiency decreases with the number of reflections giving rise to a pulsed polarization of the beam. Our study can serve as a guideline for the development

2 *Enhance. laser-induced excit. prob.*

of a polarized muonic beam for a precise measurement of the ground state hyperfine splitting of muonic hydrogen, or for μ SR experiments.

Keywords: muonic hydrogen; magnetic dipole; spin-polarization; hyperfine splitting; multipass cavity; laser propagation effect

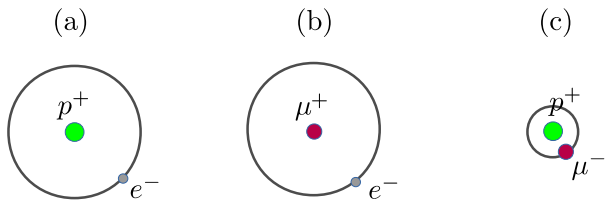
Amongst all the exotic atoms, muon (μ^\pm) prevails as the probing tool as far as the theoretical studies and experiments in atomic and nuclear physics are concerned. This is due to its relatively easier availability and longer lifetime of 2.2 μ s. Charged pion which is often the next in line amongst the exotic atoms, has a lifetime of 26 ns, making it very short-lived. Besides, unlike the pion, the muon is not influenced by the strong force of the atomic nuclei in the lattice, and hence has higher penetration depth. Muon has been studied extensively due to its relevance in the Standard model of elementary particles, and its usefulness in various applications such as μ SR experiment, and muon-catalyzed fusion, etc [1–10]. Commonly, for the application purpose of muon (whether positively or negatively charged), its kinetic energy is reduced from as high as a few MeV after being ejected from the particle accelerator, down to a few keV \sim a few eV. In this process, positive muons capture electrons to form muonium atoms while negative muons are captured by protons to form muonic hydrogen atoms. In both the cases of the recombination processes, the degree of polarization, which is 100 % upon birth, is significantly lost which needs to be spin-repolarized.

Several works have been done on obtaining slow positive muon beam [11–18]. We turn our focus on the muonic hydrogen which has proved to be a suitable candidate to precisely determine the size of proton. This is because of the proximity of the negative muon to the proton that amplifies the atomic properties of the muonic hydrogen due to the presence of the negative muon (200 times heavier particle than the electron) in the atomic orbit with a radius of about 1/200 th of that of hydrogen and muonium. For comparison, we have used the figure from our previous work [19] which summarizes the various atomic parameters of hydrogen, muonium, and muonic hydrogen in Fig. 1.

The famous study on the Lamb shift ($2S_{1/2} - 2P_{1/2}$ energy difference) of muonic hydrogen at PSI [2] reported that the proton radius is about 4% smaller than the widely accepted value. This puzzle has spearheaded many works on spectroscopy and particle physics [20–22]. Along this line, Adamczak *et al.* proposed a method of determining the proton size with accuracy by an independent measurement of the hyperfine splitting ($1S(F = 0) - 1S(F = 1)$) of the ground state of muonic hydrogen [23–25]. The $1S(F = 0) - 1S(F = 1)$ transition wavelength is in the mid-infrared range (6.76 μ m), is dipole-forbidden, and the process involves magnetic dipole transition which is several orders of magnitude weaker than the electric dipole transition. The experimental scheme was originally proposed by Bakalov *et al.* [26], in which negative muons

are slowed down and stopped in a pure hydrogen target between two parallel gold or aluminium plates to form muonic hydrogen. Recently, we also have studied the laser-induced hyperfine ground state excitation probability of Doppler-broadened muonic hydrogen for various pulse parameters that can serve as a guideline for the development of the relevant laser source, depending on whether the purpose of exciting muonic hydrogen is measuring the ground state hyperfine splitting of muonic hydrogen with precision, or producing spin-polarized muonic hydrogen beam [19]. Adamczak *et al.* have proposed a scheme of placing the target inside a multipass cavity in order to increase the excitation probability which is otherwise merely 1.2×10^{-5} (too low for the proposed experiment to be feasible) with a laser pulse of long duration at $6.76 \mu\text{m}$ with 0.25 mJ pulse energy in a single interaction of the laser pulse with the muonic hydrogen beam at a temperature of 300 K [23]. Undoubtedly, this experiment comes with huge technical challenges. From a theoretical point of view, a study of the elementary challenges such as the deterioration of the laser field profile as it propagates through the muonic hydrogen medium inside the multipass cavity for various ranges of medium densities, is essential for completeness. For the muon beam facilities around the world at present, the achievable beam density is not high enough for any laser propagation effect to arise. For example, at the J-PARC, the density of the muon beam is typically 10^5 cm^{-3} . Nevertheless, it is important to study the laser propagation effect on the polarization of the muons, as the density is increased, as might be possible by the technological development in future. Besides, the prospects and limitations in tailoring the temporal profile of the muonic hydrogen beam in such a multipass cavity setup, needs to be discussed. We note that, pulsed muon and CW muon sources that have been developed at various facilities across the world, have their own advantages and disadvantages depending upon the purpose of the muon source. For example, the PSI and TRIUMF [27, 28] are both home to intense continuous muon beam which is suitable for spectroscopy experiments, whereas KEK, RIKEN-RAL and J-PARC MUSE [29, 30] serve as the sources of pulsed muon beams which are better suited for μSR experiments. It is to be seen in this context, how the multipass cavity setup might play its role in shaping the temporal profile of the muonic hydrogen beam.

In the present work, we study the excitation probability of the muonic hydrogen by nanosecond laser pulses in a multipass cavity setup and investigate the conditions under which the excitation probability is enhanced which leads to increased polarization of muons. The bandwidth of the laser pulse we consider in our study is broader as compared to the Doppler width of the atoms. The results we present in this work would be useful in the development of experimental setup for polarized muonic beam.



	Hydrogen	Muonium	Muonic Hydrogen
Radius	$a_0 = 0.529\text{\AA}$	$\sim a_0$	$\sim a_0/200$
Ionization potential	13.6 eV	13.6 eV	2.7 keV
Hyperfine split. $1S(F = 0 - F = 1)$	1.4 GHz	4.5 GHz	44 THz

Fig. 1 (Color online) Comparison of the hydrogen and hydrogen-like systems involving positive and negative muons.

1 System Description

Figure 2 shows the schematic diagram of the system we have considered. We consider the hyperfine sublevels of the ground ($1s$) state of the muonic hydrogen. A laser beam in the mid-infrared range ($6.7\text{ }\mu\text{m}$) is shrunk by reducing its cross section by a factor k (thereby increasing the intensity by the same factor), and projected into a multipass cavity with perfect reflectivity. The muonic hydrogen beam is passed through the multipass cavity providing k reflections of the laser beam, thereby preserving the total irradiated target volume. The assumption of a multipass cavity with perfect reflectivity is for the sake of simplicity given that the intensity of the laser beam is barely attenuated by the mirrors of reflectivity as high as 99.999 % for the number of reflections considered in this work. In steady state, the slow beam of muonic hydrogen, after the fast muons being captured by the hydrogen atoms inside the cavity, can be treated to be frozen in space when compared to the laser pulse passing through the multipass cavity.

We assume a Gaussian pulse which excites the muonic hydrogen from the hyperfine singlet state, $1s(F = 0)$, to the triplet state, $1s(F = 1)$, through magnetic dipole ($M1$) interaction. We note that, the hyperfine transition is electric dipole forbidden and it is the magnetic dipole component which has the most significant contribution in the laser-matter interaction. The magnetic field of the pulse with central frequency ω is written as

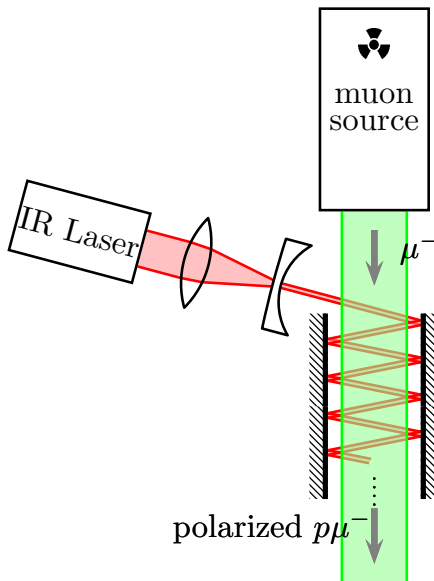


Fig. 2 (Color online) Schematic diagram showing the muonic hydrogen atoms inside a multipass cavity with mirrors of perfect reflectivity. An infrared laser pulse is shrunk in its beam cross-section and goes through a number of reflections such that the interaction volume of the muonic hydrogen and the laser pulse is preserved.

$$\mathcal{B}(t) = B(t) \exp[-i\omega t] + \text{c.c.}, \quad (1)$$

where $B(t)$ is the magnetic field amplitude of the pulse. The magnetic transition dipole moment of the muonic hydrogen atom, M , calculated by us in our previous work is $\frac{1}{\sqrt{6}} \frac{e\hbar}{2m_\mu}$ [19]. The Rabi frequency Ω , corresponding to the magnetic dipole transition in S.I. unit, is

$$\Omega(\text{ns}^{-1}) = 1.77 \times 10^{-6} \sqrt{I(t)} \quad (2)$$

where $I(t)$ is the laser intensity in units of W/cm^2 . We employ a set of Maxwell-Schrödinger equation, which can be easily obtained by coupling the probability amplitudes, a_0 and a_1 , of the hyperfine states, $1s(F = 0)$ and $1s(F = 1)$, respectively and Maxwell's equations, which reads

$$\frac{\partial}{\partial t}a_0(z, t) = i\Omega^*(z, t)a_1(z, t), \quad (3)$$

$$\frac{\partial}{\partial t}a_1(z, t) = i\Omega(z, t)a_0(z, t), \quad (4)$$

$$\frac{\partial}{\partial z}\Omega(z, t) = -2i\alpha a_1^*(z, t)a_0(z, t). \quad (5)$$

where $\alpha = N\omega M^2\mu_0c/2$, is defined as the laser propagation coefficient of the muonic hydrogen medium, N being the density of the medium [31]. While obtaining the above equations, we have neglected the spontaneous decay rate of the muonic hydrogen for the range of time duration considered. Although the slow muonic hydrogen atoms formed are unpolarized, i.e. 50% of the atoms are in the state $1s(F = 0)$ and 50% are in state $1s(F = 1)$, the initial condition that all the atoms are in the singlet state, $1s(F = 0)$, simplifies the study without the loss of generality. We numerically calculate the Doppler-averaged spin-flip probability, P , of the ground hyperfine state, from $1S(F = 0)$ to $1S(F = 1)$, of the muonic hydrogen, taking into account the laser propagation effect of the medium on the laser pulse as it passes through the multipass cavity.

2 Results and Discussions

At the outset, it should be noted that we confine our study to a peak intensity, $I_0 = 1 \times 10^6$ W/cm² and a duration, $\tau = 2$ ns of the laser pulse. At resonance, the Doppler-averaged spin-flip probability of the muonic hydrogen atoms at 10 K, is enhanced by a factor of 2.3 as compared to that at 300 K. The lowest temperature the system can go is 10 K as below which molecular $p\mu\mu$ are formed. Hence, we also confine our study to the muonic hydrogen medium at a temperature of 10 K. Additionally, at 10 K, the Doppler broadening of the medium is about 100 MHz which is less than half of the bandwidth of a 2 ns pulse, namely 220 MHz. As the bandwidth of the pulse covers the Doppler width of the medium fairly enough, we can safely calculate the spin-flip probability at resonance without taking the Doppler average and apply a Gaussian window function with the parameters equal to that of the laser pulse to effectively calculate the Doppler-averaged spin-flip probability, P at 10 K, which saves computation time, without loss of accuracy. In Fig. 3 (a), we show the normalized Doppler distribution of muonic hydrogen atoms at 300 K and 10 K, with blue and green solid lines, respectively. The area under each of the lines are unity. In Fig. 3 (b), we show the normalized Doppler distribution multiplied with a Gaussian window function of width 220 MHz. The areas, S_{10K} (= 0.917) and S_{300K} (= 0.387), of the modified distribution

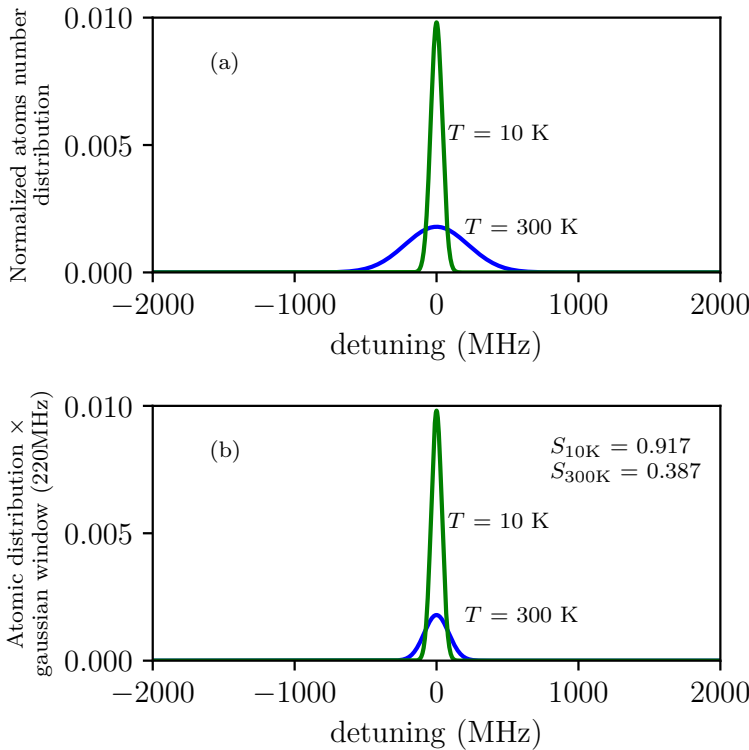


Fig. 3 (Color online) (a) Normalized distribution of the number of Doppler-broadened muonic hydrogen atoms at a temperature of 300 K (blue line) and 10 K (green line). The area under each of the lines is unity. (b) Same as panel (a) multiplied with a Gaussian window function of width 220 MHz, which corresponds to the spectral width of a 2 ns Gaussian pulse. The ratio of the areas under the green and red line is $0.917/0.387 = 2.3$.

lines in Fig. 3 (b) represent the number of atoms covered by the bandwidth of the laser pulse at temperatures 10 K and 300 K, respectively. The ratio of S_{10K} and S_{300K} turns out to be 2.3, which is exactly what we have calculated by using the amplitude equations of the states and averaging over the Doppler distribution of the atoms. This validates our proposed method of calculation. Henceforth, in this work, P is simply equal to the population of the ground hyperfine state, $1s(F = 1)$.

We consider a 30 cm long cavity with a width of 10 mm which accommodates approximately 100 reflections ($k = 100$) with an angular incidence of the laser pulse at an angle of 10 degrees as clear from Fig. 2. It is more convenient to use k instead of the otherwise commonly used, optical depth, αz , where z is the geometrical depth that the pulse traverses inside the medium. Typical value of the density of the muonic hydrogen atoms, N , in the cavity, after the slow down process and losses by transfer of muons to heavier nucleus

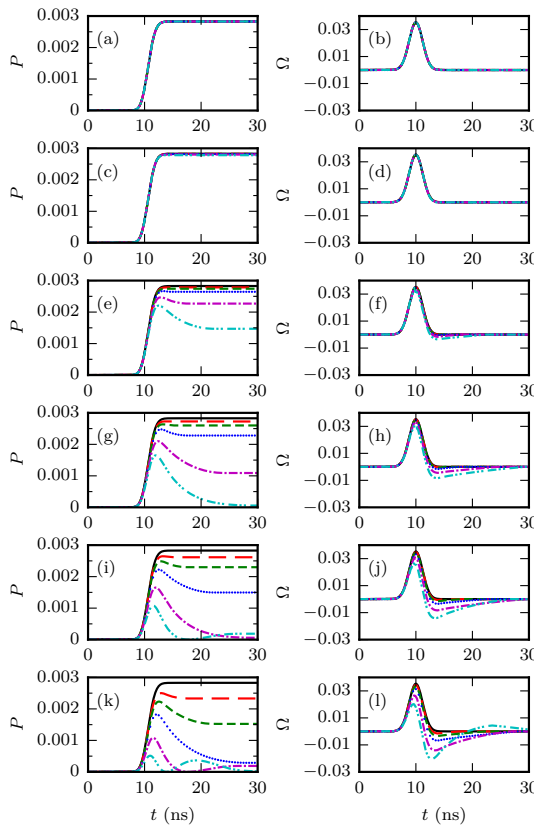


Fig. 4 (Color online) Temporal variation of the population of the ground hyperfine state, $1s(F = 1)$ and the laser field, Ω with the medium propagation coefficient, $\alpha = 4 \times 10^{-18} \text{ mm}^{-1}$ [(a), (b)], $4 \times 10^{-6} \text{ mm}^{-1}$ [(c), (d)], $4 \times 10^{-5} \text{ mm}^{-1}$ [(e), (f)], $1 \times 10^{-4} \text{ mm}^{-1}$ [(g), (h)], $2 \times 10^{-4} \text{ mm}^{-1}$ [(i), (j)], and $4 \times 10^{-4} \text{ mm}^{-1}$ [(k), (l)], at different reflection numbers, $k = 1$ (black solid line), 5 (red long-dashed line), 10 (green short-dashed line), 20 (blue dotted line), 50 (magenta dot-dashed line), and 100 (cyan double dot-dashed line). The laser pulse intensity is $1 \times 10^6 \text{ W/cm}^2$ and the pulse duration is 2 ns for all the graphs.

from the proton, is about 10^5 cm^{-3} which is equivalent to a propagation coefficient, $\alpha = 4 \times 10^{-18} \text{ mm}^{-1}$. At first glance, this is extremely low to cause any propagation effect on the laser pulse for the ranges of optical depths the pulse traverses inside the cavity. We calculate the representative values at the midpoint of each path between the mirrors, corresponding to k . In Fig. 4, we study the time evolution of the population of the state $1s(F = 1)$, P and temporal variation of the laser field, Ω for increasing values of propagation coefficients, α down the columns. In each panel, we show the representative values at $k = 1, 5, 10, 20, 50$, and 100 with black solid, red long-dashed, green

short-dashed, blue dotted, magenta dot-dashed, and cyan double dot-dashed lines, respectively. Panels (a), (c), (e), (g), (i), and (k) [(b), (d), (f), (h), (j), and (l)] show the temporal variation of $P(\Omega)$ for $\alpha = 4 \times 10^{-18}$, 4×10^{-6} , 4×10^{-5} , 1×10^{-4} , 2×10^{-4} , and 4×10^{-4} mm⁻¹, respectively. Figure 4 (a) shows that P increases by two orders of magnitude due to shrinking of the cross-section of the laser pulse. It remains same through out the optical path of the pulse as the laser field, Ω is unaffected due to the low muon density. By observing the Eqs. 3-5, we note that it is the interplay between the pulse area $\sim \Omega\tau$ and the optical path, αz which dictates the laser propagation effect on the dynamics of the system.

The results remain the same as Fig. 4 (a) and (b) for the range of values of α until it increases to 4×10^{-6} mm⁻¹ for which temporal variation of P and Ω just barely change with k . This is because, in that region of α , $\Omega\tau \gg \alpha z$, hence Ω effectively remains constant. This implies that in this range of α , P remains uniform through out the cavity as the muonic hydrogen atoms are sparsely populated inside the cavity. Therefore, we skip the results for those values of α and start from $\alpha = 4 \times 10^{-6}$ mm⁻¹ ($N = 10^{17}$ cm⁻³) from Fig. 4 (c) and (d). Undoubtedly, for $\alpha = 4 \times 10^{-6}$ mm⁻¹, αz begins to approach $\Omega\tau$, $\alpha z = 0.0004\Omega\tau$, to be specific. In Fig. 4 (e) and (f) where $\alpha = 4 \times 10^{-5}$ mm⁻¹ ($N = 10^{17}$ cm⁻³), P starts to fall appreciably below 0.0028 and Ω begins to modulate and exhibit negative amplitude as the optical depth increases. As α further increases by a factor of two as shown in the subsequent rows in Fig. 4 (h) and (j), Ω is significantly distorted during the propagation, and the laser pulse breaks up into sub-pulses. For further higher value of α ($= 4 \times 10^{-6}$ mm⁻¹), as shown in Fig. 4 (l), Ω breaks up into sub-pulses with positive and negative amplitudes at $k = 100$. Similarly, as shown in Fig. 4 (g), (i) and (k), P saturates at values lower than 0.0028 and exhibits Rabi oscillation as optical depth increases. We note that, if the pulse area and the pulse duration is much shorter than the spontaneous decay time which is 2.2 μ s, the propagation of the laser pulse follows a non-Beer's law decay profile and propagates for much greater optical depths as compared to CW laser fields. We expect more distortion if α increases further. Clearly, the polarization of the muonic hydrogen falls off with increased propagation depth or higher value of k , with a wiggly behavior due to the modulation of Ω as k increases, as clear from Fig. 4 (i) and (k) at $t = 30$ s.

To get a clear profile of the polarization of muonic hydrogen atoms inside the cavity, in Fig. 5 (a) and (b), we plot the variation of P and the total efficiency, Q as a function of k , respectively. We define the total efficiency at a given value of k as the ratio of the total number of excited atoms to the total number of atoms in the interaction volume between $k = 0$ to the given value of k , i.e.,

$$Q = \frac{\int_k P_k N a dz}{\int_k N a dz}. \quad (6)$$

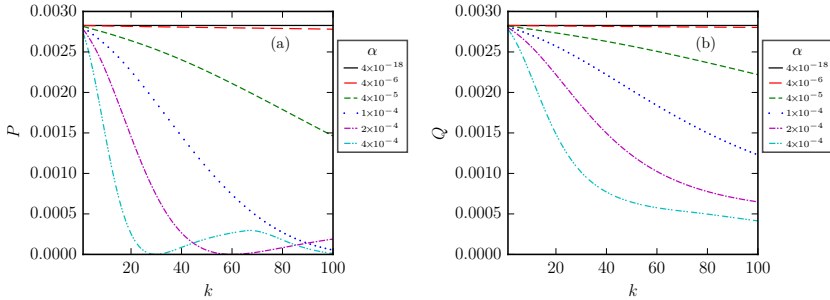


Fig. 5 (Color online) (a) Variation of the population of the ground hyperfine state, P , (b) variation of the total efficiency, Q with the reflection number, k for medium propagation coefficient, $\alpha = 4 \times 10^{-18} \text{ mm}^{-1}$ (black solid line), $4 \times 10^{-6} \text{ mm}^{-1}$ (red long-dashed line), $4 \times 10^{-5} \text{ mm}^{-1}$ (green short-dashed line), $1 \times 10^{-4} \text{ mm}^{-1}$ (blue dotted line), $2 \times 10^{-4} \text{ mm}^{-1}$ (magenta dot-dashed line), and $4 \times 10^{-4} \text{ mm}^{-1}$ (cyan double dot-dashed line).

In the above equation, P_k is the value of P at the optical depth corresponding to k , N is the density of muonic hydrogen atoms and a is the beam cross-sectional area after shrinking of the beam cross-section. In panel (a)[(b)], we plot the values of P (Q) for $\alpha = 4 \times 10^{-18}$, 4×10^{-6} , 4×10^{-5} , 1×10^{-4} , 2×10^{-4} , and 4×10^{-4} by black solid, red long-dashed, green short-dashed, blue dotted, magenta dot-dashed, and cyan double dot-dashed lines, respectively. As shown in Fig. 5 (a), P falls off rapidly as α increases beyond 4×10^{-6} and has a wiggly behavior for higher values of α as shown by the magenta dot-dashed line and cyan double dot-dashed line in Fig. 5 (a). This is due to the oscillatory behavior of Ω at higher values of α . Total efficiency, Q also falls off in a similar trend but, the wiggly behavior is absent due to the cumulative averaging of P over the range of k starting from the entrance of the cavity, as shown in Fig. 5 (b). Q at a certain k gives the ratio of the total number of excited atoms to the total number of atoms in a target volume accommodating k reflections with the beam cross-section shrunk by a factor k . Indeed, Q as a function of k provides information on how the total efficiency varies as we shrink the laser beam cross-section and accordingly increase the depth of the multipass cavity keeping the target volume fixed.

Before closing the discussion, we note that upto a fairly high density of the muonic hydrogen atoms for the given pulse area of the laser, we can obtain a uniformly polarized muonic beam with increased efficiency by employing a multipass cavity. The so-called threshold density of the muonic hydrogen will further rise if we employ a pulse with higher pulse area. By tailoring the pulse area and repetition rate, we can construct the polarized muonic beam to be continuous or periodic depending on the requirement of the experiment. Keeping the pulse area lower than the total optical depth, we can construct a pulsed polarized muonic hydrogen beam. Lastly, although the spin-flip probability of the muonic hydrogen atoms decreases down the cavity for higher

densities of the atoms, the total number of atoms excited in the interaction volume is always higher for higher density of the atoms.

3 Conclusion

In conclusion, we have studied the prospects of enhancement of the laser-induced spin-flip probability between the hyperfine ground states of Doppler-broadened muonic hydrogen by placing a multipass cavity at a temperature of 10 K. We have investigated the effect of propagation of the laser pulse in the medium of muonic hydrogen atoms inside the multipass cavity for a range of densities of the atoms. Assuming a pulse intensity of 1×10^6 W/cm² and pulse duration of 2 ns, we considered the case of shrinking the beam cross-section by a factor of 100 and employing a multipass cavity which allows 100 reflections of the pulse, preserving the total interaction volume. This transition is dipole-forbidden, and it is the magnetic dipole interaction that induces the transition. For densities of muonic hydrogen atoms ranging from 10^5 to $\sim 10^{17}$ cm⁻³, the propagation effect is totally negligible and the spin-flip probability remains uniform through out the cavity and the total efficiency is 0.0028, i.e. enhanced by two orders of magnitude. This gives rise to a uniformly polarized muon beam. As density increases beyond $\sim 10^{17}$ cm⁻³, the propagation effect can no longer be neglected and spin-flip probability is non-uniform inside the cavity. The total efficiency decreases as the pulse undergoes more reflections inside the cavity and eventually becomes 0.00041 after 100 reflections. This, in turn gives rise to a pulsed polarized muonic beam. The result we have presented will serve as a guideline for arranging muonic beams depending on the requirement of a uniform or pulsed polarized muons in μ SR experiments.

Acknowledgement

We acknowledge the helpful comments and suggestions of Dr. Parvendra Kumar, IIT Chennai, India.

Competing interests

The authors declare that there they have no competing interests.

Funding

Part of this work was funded by Rashtriya Uchchatar Shiksha Abhiyan (RUSA 2.0), MHRD, Govt. of India.

References

[1] T.P. Gorringe, D.W. Hertzog, “Precision muon physics,” Prog. Part. Nucl. Phys. **84**, 73 (2015).

12 *Enhance. laser-induced excit. prob.*

- [2] R. Pohl, A. Antognini, F. Nez, *et al.*, “The size of the proton,” *Nature* **466**, 213 (2010).
- [3] A. Antognini, F. Nez, *et al.*, “Proton Structure from the Measurement of 2S-2P Transition Frequencies of Muonic Hydrogen,” *Science* **339**, 6118, 417-420 (2013).
- [4] P. Bakule, and E. Morenzoni, “Generation and applications of slow polarized muons,” *Contemporary Physics* **45:3**, 203-225 (2004).
- [5] J. P. Miller, E. de Rafael, and B. L. Roberts, “Muon (g-2) experiment and theory,” *Rep. Prog. Phys.* **70**, 795-881 (2007).
- [6] T. Lancaster, S. J. Blundell, P. J. Baker, M. L. Brooks, W. Hayes, F. L. Pratt, J. L. Manson, M. M. Conner, and J. A. Schlueter, “Muon-Fluorine Entangled States in Molecular Magnets,” *Phys. Rev. Lett.* **99**, 267601 (2007).
- [7] A. Bungau, R. Cywinski, C. Bungau, P. King, and J. S. Lord, “Target optimization studies for surface muon production,” *Phys. Rev. ST Accel. Beams* **17**, 034701 (2014).
- [8] S. Nagamiya, K. Nagamine, O. Hashimoto, and T. Yamazaki, “Negative-muon spin rotation at the oxygen site in paramagnetic MnO⁺,” *Phys. Rev. Lett.* **35**, 308–311 (1975).
- [9] P. Dalmas de Réotier and A. Yaouanc, “Muon spin rotation and relaxation in magnetic materials,” *J. Phys. Condens. Matter* **9**, 9113–9166 (1997).
- [10] D. V. Balin, V. A. Ganzha, S. M. Kozlov, E. M. Maev, G. E. Petrov, M. A. Soroka, G. N. Schapkin, G. G. Semenchuk, V. A. Trofimov, A. A. Vasiliev, A. A. Vorobyov, N. I. Voropaev, C. Petitjean, B. Gartner, B. Lauss, J. Marton, J. Zmeskal, T. Case, K. M. Crowe, P. Kammel, F. J. Hartmann, M. P. Faifman, “High precision study of muon catalyzed fusion in D₂ and HD gas,” *Phys. Particles and Nuclei* **42**, 185–214 (2011).
- [11] K. Nagamine, Y. Miyake, K. Shimomura, P. Birrer, J. P. Marangos, M. Iwasaki, P. Strasser, and T. Kuga “Ultraslow Positive-Muon Generation by Laser Ionization of Thermal Muonium from Hot Tungsten at Primary Proton Beam,” *Phys. Rev. Lett.* **74**, 4811 (1995).
- [12] E. Morenzoni, F. Kottmann, D. Maden, B. Matthias, M. Meyberg, Th. Prokscha, Th. Wutzke, and U. Zimmermann, “Generation of very slow polarized positive muons,” *Phys. Rev. Lett.* **72**, 2793 (1995).
- [13] P. Bakule, Y. Matsuda, Y. Miyake, P. Strasser, K. Shimomura, S. Makimura, and K. Nagamine, “Slow muon experiment by laser resonant

ionization method at RIKEN-RAL muon facility,” *Spectrochim. Acta Part B* **58**, 1019–1030 (2003).

- [14] G. A. Beer, Y. Fujiwara, S. Hirota, K. Ishida, M. Iwasaki, S. Kanda, H. Kawai, N. Kawamura, R. Kitamura, S. Lee, W. Lee, G. M. Marshall, T. Mibe, Y. Miyake, S. Okada, K. Olchanski, A. Olin, H. Ohnishi, Y. Oishi, M. Otani, N. Saito, K. Shimomura, P. Strasser, M. Tabata, D. Tomono, K. Ueno, E. Won, and K. Yokoyama, “Enhancement of muonium emission rate from silica aerogel with a laser-ablated surface,” *Prog. Theor. Exp. Phys.* **2014**, 091C01 (2014).
- [15] T. Nakajima, “A scheme to polarize nuclear-spin of atoms by a sequence of short laser pulses: application to the muonium,” *Opt. Express* **18**, 27468–27480 (2010).
- [16] T. Nakajima, “Spin polarization of Doppler-broadened atoms by the broadband nanosecond and transform-limited picosecond laser pulses: case study for the muonium,” *J. Opt. Soc. Am. B* **29**, 2420–2424 (2012).
- [17] R. M. Das, S. Chatterjee, M. Iwasaki, and T. Nakajima, “Ionization efficiency of Doppler-broadened atoms by transform-limited and broadband nanosecond pulses: one-photon resonant two-photon ionization of muoniums,” *J. Opt. Soc. Am. B* **32**, 1237–1244 (2015).
- [18] R. M. Das, K. Ishida, M. Iwasaki, and T. Nakajima, “Nuclear-spin polarization of atoms by chirped laser pulses: application to the muonium,” *J. Opt. Soc. Am. B* **35**, 1799–1810 (2018).
- [19] R. M. Das, K. Ishida, M. Iwasaki, and T. Nakajima, “Excitation probability of the hyperfine ground state of Doppler-broadened muonic hydrogen through dipole-forbidden transition,” *Optik* **200**, 163380 (2020).
- [20] S. Yamamoto, K. Ninomiya, N. Kawamura, T. Yabe, and Y. Hirano, “Three-dimensional (3D) optical imaging of muon beam using a plastic scintillator plate in water,” *Nucl. Instrum. Meth. A* **1015**, 165768 (2021).
- [21] L. Serafini and I. Drebot and A. Bacci and F. Broggi and C. Curatolo and A. Marocchino and N. Panzeri and V. Petrillo and A.R. Rossi and M. Rossetti Conti, “A muon source based on plasma accelerators,” *Nucl. Instrum. Meth. A* **909**, 309-313 (2018).
- [22] The future prospects of muon colliders and neutrino factories. <http://www.osti.gov/servlets/purl/1572287>.
- [23] A. Adamczak, D. Bakalov, L. Stoychev, and A. Vacchi, “Hyperfine spectroscopy of muonic hydrogen and the PSI Lamb shift experiment,” *Nucl. Instrum. Meth. B* **281**, 72-76 (2012).

14 *Enhance. laser-induced excit. prob.*

- [24] J.R. Sapirstein, J.R. Yennie, in: T. Kinoshita, Quantum Electrodynamics, World Scientific, 560 (1990).
- [25] M.I. Eides, H. Grotch, V.A. Shelyuto, “Theory of light hydrogenlike atoms.” Phys. Rep. **342**, 62 (2001).
- [26] D. Bakalov, E. Milotti, C. Rizzo, A. Vacchi, and E. Zavattini, “Experimental method to measure the hyperfine splitting of muonic hydrogen (μp)1S,” Phys. Lett. A **172**, 277 (1993).
- [27] F. Foroughi, E. Morenzoni, T. Prokscha, *et al.*, “Upgrading the PSI Muon Facility,” Hyperfine Interactions **138**, 483—488 (2001).
- [28] H.K. Walter, “Muon Physics at the Paul Scherrer Institut (psi) and at Triumf,” High Intensity Muon Sources - Kek International Workshop, World Scientific Publishing Co. Pte. Ltd, 279–290 (2001).
- [29] T. Matsuzaki, K. Ishida, K. Nagamine, I. Watanabe, G.H. Eaton, and W.G. Williams, “The RIKEN-RAL pulsed Muon Facility,” Nucl. Instrum. Meth. A **465**, 365–383 (2001).
- [30] Y. Miyake, K. Shimomura, N. Kawamura, P. Strasser, A. Koda, S. Makimura, H. Fujimori, Y. Ikeda, K. Nakahara, S. Takeshita, M. Kato, K. Kojima, Y. Kobayashi, K. Nishiyama, R. Kadono, W. Higemoto, T. U. Ito, K. Ninomiya, K. Kubo, and K. Nagamine, “J-PARC Muon Facility, MUSE,” Phys. Proc. **30**, 46–49 (2012).
- [31] G. Buica, T. Nakajima, “Propagation of two short laser pulse trains in a Λ -type three-level medium under conditions of electromagnetically induced transparency,” Opt. Comm. **332**, 59–69 (2014).